Vibrationally inelastic H + D_2 collisions are forward-scattered

Noah T. Goldberg[a], Jianyang Zhang[a], Konrad Koszinowski[a,1], Foudhil Bouakline[b], Stuart C. Althorpe[b], and Richard N. Zare[a,2]

[a]Department of Chemistry, Stanford University, Stanford, CA 94305-5080; and [b]Department of Chemistry, University of Cambridge, Cambridge CB2 1EW, United Kingdom

Edited by Dudley R. Herschbach, Harvard University, Cambridge, MA, and approved October 14, 2008 (received for review August 11, 2008)

We have measured differential cross sections (DCSs) for the vibrationally inelastic scattering process H + *o*-D_2(v = 0, j = 0,2) → H + *o*-D_2(v' = 1–4, j' even). Several different collision energies and nearly the entire range of populated product quantum states are studied. The products are dominantly forward-scattered in all cases. This behavior is the opposite of what is predicted by the conventional textbook mechanism, in which collisions at small impact parameters compress the bond and cause the products to recoil in the backward direction. Recent quasiclassical trajectory (QCT) calculations examining only the *o*-D_2(v' = 3, j') products suggest that vibrationally inelastic scattering is the result of a frustrated reaction in which the D—D bond is stretched, but not broken, during the collision. These QCT calculations provide a qualitative explanation for the observed forward-scattering, but they do not agree with experiments at the lowest values of j'. The present work shows that quantum mechanical calculations agree closely with experiments and expands upon previous results to show that forward-scattering is universally observed in vibrationally inelastic H + D_2 collisions over a broad range of conditions.

fully quantum calculations | ion imaging | reaction dynamics | vibrationally inelastic scattering

The hydrogen exchange reaction, H + H_2 → H_2 + H, as the prototypic model system in the study of reaction dynamics, has garnered much attention from experimentalists and theoreticians alike. Dozens of studies over the past few decades have compared measurements of integral and differential cross sections (ICSs and DCSs) for reactive scattering with the results of quasiclassical trajectory (QCT) and quantum mechanical (QM) calculations; several excellent reviews have been published recently (1–3). Despite a few remaining slight discrepancies that possibly result from errors in these challenging experiments (4, 5), the agreement between recent experiments and calculations is nearly perfect (6–9), suggesting that reactive scattering in this fundamental reaction is well understood. In contrast to the wealth of information available for the reactive channel, only a handful of studies have focused on the vibrationally inelastic scattering channel (1, 10–16), and only one of these presented rotational-state-selected DCSs (16).

For the H + D_2 isotopic variant, 1 quantum of D_2 vibration is roughly equivalent in energy to the reaction barrier to form HD on the minimum energy path (≈0.4 eV), and the nuclear motion involved in D_2 vibration is qualitatively similar to the lengthening of the D—D bond that occurs near the transition state in a reactive collision. Indeed, inelastic scattering trajectories may recross the reaction barrier multiple times (1, 13, 16, 17). Reactive collisions are dominated by direct recoil at small impact parameters (1, 18, 19), but nonreactive collisions comprise a much larger range of impact parameters and may sample quite different regions of the potential energy surface (PES). Studying inelastic collisions in which a large amount of translational energy is transferred to internal energy can provide complementary information which, when combined with reactive scattering data, can give a more complete picture of the dynamics of the H + D_2 system.

Recently, our observation that the inelastic scattering process H + *o*-D_2($v = 0, j = 0,2$) → H + *o*-D_2($v' = 3, j'$ even) is primarily forward-scattered led to the discovery of a tug-of-war mechanism (16). In tug-of-war collisions, the H atom pulls on the nearest D atom but fails to capture it to form the HD molecule. In the process, stretching of the D—D bond leads to highly excited D_2. This behavior is contrary to the previously accepted wisdom that back-scattered direct recoil collisions are required to compress the D—D bond and induce vibration (20). In the present experiments, we map the inelastic scattering DCS as a function of v', j' and collision energy and show that forward-scattering is a general feature of vibrationally inelastic H + D_2 collisions. New QM calculations are in close agreement with these measurements, and we suggest that tug-of-war collisions may be important in other chemical systems in which temporary bond formation occurs.

Results

A total of 19 DCSs [summarized in supporting information (SI) Table S1] were measured for the collision process H + D_2 → H + D_2(v', j'). Two types of reactants, *o*-D_2 (j even) and *p*-D_2 (j odd), are present in the statistical ratio 2:1. The probability of converting between *o*-D_2 and *p*-D_2 in an inelastic collision is negligible, and the inelastic scattering cross-section is found to be identical for *o*-D_2 and *p*-D_2 by both experiment and calculation (15). Because preliminary measurements of DCSs for D_2(v' = 1, j') revealed no obvious differences between even and odd j', in the present work, we focus on even j' for 2 reasons: (*i*) higher signal levels because more *o*-D_2 than *p*-D_2 is present and (*ii*) the *o*-D_2 is rotationally colder than the *p*-D_2 (average E_{rot} = 0.019 eV for the former, and 0.025 eV for the latter). The ideal state-to-state experiment would involve only ground-state reactants; in the present experiment, the j = 0:j = 2 ratio is roughly 1:1, and only a few percent of the population is in $j \geq 4$.

Most of the DCSs were measured at a collision energy of E_{coll} = 1.72 eV, but several DCSs were measured at various energies between $1.58 \leq E_{coll} \leq 1.94$ eV. Large background was encountered for the v' = 1 experiments, especially for low values of j', and DCSs could be obtained only for $j' \geq 4$. The DCS appeared to change smoothly between neighboring j' values, so

Author contributions: N.T.G., J.Z., K.K., F.B., S.C.A., and R.N.Z. designed research; N.T.G., J.Z., K.K., F.B., and S.C.A. performed research; N.T.G. analyzed data; and N.T.G. wrote the paper.

The authors declare no conflict of interest.

This article is a PNAS Direct Submission.

[1]Present address: Department Chemie und Biochemie, Ludwig-Maximilians-Universität München, Butenandtstrasse 5-13, Haus F, 81377 Munich, Germany.

[2]To whom correspondence should be addressed at: S. G. Mudd Building, Room 133, 333 Campus Drive, Stanford, CA 94305-5080. E-mail: zare@stanford.edu.

This article contains supporting information online at www.pnas.org/cgi/content/full/0807942105/DCSupplemental.

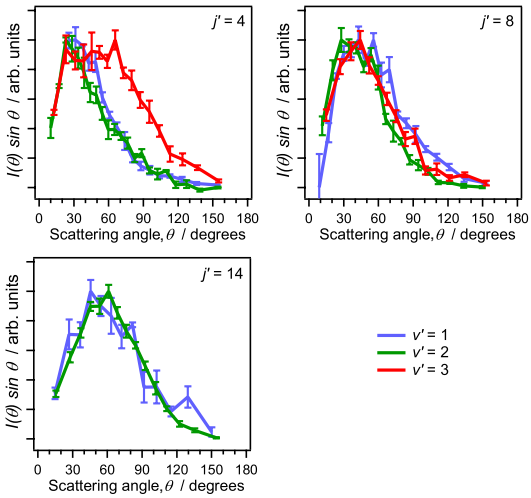

Fig. 1. Differential cross sections $I(\theta)\sin\theta$ for $D_2(v' = 1, j' = 4,8,14)$ products formed at $E_{coll} = 1.76$, 1.73, and 1.65 eV, respectively (blue lines), and $D_2(v' = 2, j' = 4,8,14)$ products formed at $E_{coll} = 1.72$ eV (green lines), scaled so that the maximum intensity is unity. Also shown for comparison are data for $D_2(v' = 3, j' = 4)$ (see Fig. 2) and $D_2(v' = 3, j' = 8)$ at $E_{coll} = 1.72$ eV. The scattering angle θ is defined so that 0° corresponds to perfect forward-scattering (no deflection) of each collision partner. Error bars represent 1 standard deviation.

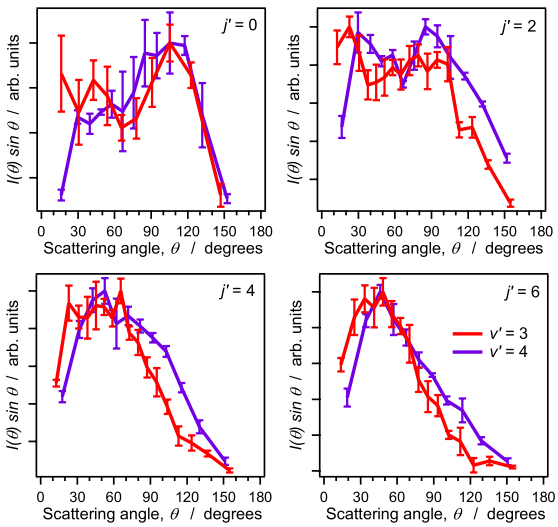

Fig. 2. Differential cross sections $I(\theta)\sin\theta$ for $D_2(v' = 3, j' = 0,2,4,6)$ products formed at $E_{coll} = 1.72$ eV (red lines) and $D_2(v' = 4, j' = 0,2,4,6)$ products formed at $E_{coll} = 1.82$ eV (purple lines), scaled so that the maximum intensity is unity. The scattering angle θ is defined so that 0° corresponds to perfect forward-scattering (no deflection) of each collision partner. Error bars represent 1 standard deviation.

$j' = 4,8,14$ were chosen as representatives of low, moderate, and high rotational excitation with acceptable signal-to-background ratios. The same values of j' were also used for $v' = 2$, so that the DCSs for these 2 vibrational manifolds can be directly compared. D_2 products with $v' = 3$ and $v' = 4$ were too rotationally cold to allow us to obtain DCSs for $j' > 8$ and $j' > 6$, respectively. Instead, we measured the DCSs for all of the even rotational states in the $v' = 3$ and 4 manifolds that had observable populations.

The dependence of the DCS on j' is different for low vs. high vibrational excitation of D_2. Fig. 1 illustrates this behavior for the former situation, $D_2(v' = 1,2)$. Most of the intensity is in the forward-scattered hemisphere; low values of j' have narrow forward-scattered peaks with long tails, and the peaks broaden and shift toward sideward-scattering as j' increases. There is essentially no difference between $v' = 1$ and $v' = 2$ within the uncertainty of the measurement. For large values of j', the DCS is similar to what is observed for $v' = 3$: note that the DCS for $D_2(v' = 3, j' = 8)$ shown in Fig. 1 is virtually indistinguishable from those for $v' = 1$ and 2. In contrast, for $j' \leq 4$, the peak is significantly broader for large v' (also see comparison of $j' = 4$ in Fig. 2).

Fig. 2 presents the DCSs for different j' values of $D_2(v' = 3,4)$. For $j' = 6$ there is a single forward-scattered peak, and a second sideward-scattered peak grows in as j' decreases. The differences between $v' = 3$ and $v' = 4$ are small, although $v' = 4$ is slightly more back-scattered for all values of j'. The collision energy was increased from 1.72 eV to 1.82 eV for the $v' = 4$ experiments to help increase the signal in compensation for smaller cross-sections, but this does not affect the comparison significantly (as will be discussed). The collision energy dependence of the DCS for $D_2(v' = 3, j' = 2,4,8)$ is presented in Fig. 3. Only small variations are seen over the range $1.58 \leq E_{coll} \leq 1.94$ eV. The distribution becomes slightly more forward-scattered as the collision energy increases, although the difference is barely larger than the statistical error.

Discussion

Overview. It has long been accepted that vibrational energy transfer in a neutral–neutral collision between an atom and a diatomic molecule occurs primarily by compressing the bond. The situation is analogous to hitting a spring with a hammer: Low-impact-parameter collisions are required, in which the incident atom has a large velocity component along the bond axis of the molecule. Such collisions necessarily lead to recoil of both atom and molecule in the reverse of their initial directions. Forward-scattering is associated with glancing collisions at large impact parameters, and these collisions are not expected to couple energy into vibration effectively.

Surprisingly, we observed that in $H + o\text{-}D_2(v = 0, j = 0,2) \rightarrow H + o\text{-}D_2(v' = 3, j')$ collisions, most of the vibrationally excited D_2 products are scattered in the forward direction (16). QCT calculations indicate that for collisions with small impact parameters, the reactants approach in a nearly collinear geometry,

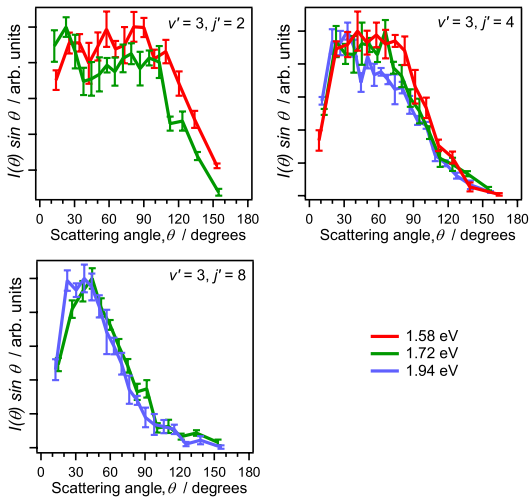

Fig. 3. Differential cross sections $I(\theta)\sin\theta$ for $D_2(v' = 3, j' = 2,4,8)$ products formed at $E_{coll} = 1.58$ eV (red lines), 1.72 eV (green lines), and 1.94 eV (blue lines), scaled so that the maximum intensity is unity. The scattering angle θ is defined so that 0° corresponds to perfect forward-scattering (no deflection) of each collision partner. Error bars represent 1 standard deviation.

and the products scatter backward. These trajectories compete with the collinear direct-recoil mechanism that dominates the reactive scattering process. This picture seems consistent with conventional wisdom, but close examination of the trajectories reveals that the impact of the H atom never compresses the D—D bond, although on closest approach, a repulsive force arises between H and the closest D atom. It seems that the incident H atom stabilizes the nearest D atom at the turning point of the D_2 vibration, and the system undergoes half of a symmetric stretch as the H atom departs. This causes the 2 D atoms to snap back together with increased vibrational excitation. Many trajectories, roughly 2/3 of $D_2(v' = 3)$ products, cross the reaction barrier several times. This fact suggests that inelastic scattering arises from a frustrated reaction in which the H atom fails to capture the nearest D atom to form HD. For collisions at higher impact parameters, the trajectories tend to be more direct (noncrossing) in character. The reactants approach in a nearly perpendicular geometry, and the incident H atom has a near-zero velocity component along the D—D bond. The bend angle of the H—D—D complex changes rapidly, and as the H atom passes through the collinear attractive well, it begins to tug the nearest D atom. The D—D bond is subsequently stretched to induce vibrational energy transfer. In some cases, this can occur without appreciable deflection of the reactants from their initial paths of motion, leading to forward-scattering near 0°. Crossing and noncrossing trajectories can each scatter into a wide range of angles, however, so there is a gradual progression rather than a strict cutoff between mechanisms for forward- vs. backward-scattering. Because the D—D bond is stretched, not compressed, in both forward scattered and backward-scattered trajectories, we suggested the term ''tug of war'' to describe the frustrated reaction mechanism that leads to vibrational excitation.

In the present work we seek to extend our earlier experiments to determine whether the tug-of-war mechanism is unique to the $D_2(v' = 3)$ channel or if it represents general behavior. The experiment cannot distinguish between multiple mechanisms that cause scattering into the same angle and thus cannot differentiate between the influences of attractive and repulsive forces or between crossing and noncrossing mechanisms. Nonetheless, similarities between the present observations and previous work can (and do) suggest that the same basic tug-of-war mechanism is operative.

Sources of Error. The experiments are technically challenging, with small signal levels and strong background; several sources of contamination are also present and may introduce systematic error. What follows is a detailed discussion of these sources of error.

Resonant and Nonresonant D_2 Background. We use a UV laser pulse to initiate the collision process and a second UV laser pulse to effect [2 + 1] resonance-enhanced multiphoton ionization (REMPI) for detection of $D_2(v', j')$ products. The inelastic scattering cross-sections are small, so background from nonresonantly ionized $D_2(v = 0)$, the primary component of our jet-cooled molecular beam, poses a particular challenge. These ions are translationally cold and in some cases can obscure the signal from slow-moving products (corresponding to forward-scattering in the DCS). As shown in Fig. S1, for $v' \geq 2$, we are able to subtract the nonresonant background peak that appears at speeds below $\approx$1 km s^{-1}. The probe laser can also create new products during the duration of its pulse. This background appears at higher speeds and overlaps the allowed speed range of the desired signal, but modulating the delay between the 2 laser pulses allows us to isolate and retain only the signal that depends on both lasers.

For $v' = 1$, a much larger background with both resonant and nonresonant components is present. We were able to subtract nearly all of the background by using 2-color Doppler-free REMPI (21), but the remaining signal was only a few hundred ions per day, and long-term drift prevented us from measuring DCSs. Ultimately, we were forced to scan the wavelength of a single laser over the Doppler line width and measure the signal resulting from the probe laser alone, which we normally consider to be unwanted background. This approach limits us to a single collision energy, which changes slightly with j' because the REMPI wavelength is different for each rotational level. The nonresonant background was subtracted by detuning the laser from the REMPI line and collecting background for the same duration as the scan, with all other conditions held constant. Resonant background still contaminates the measurement as shown in Fig. S1 but, fortuitously, the majority of the background is outside the range of speeds that can contribute to the desired signal in most cases. Space charge effects from these background ions are not expected to blur the image because, even in the worst case, the total count rate is still $<$1 ion per laser shot. In other cases, the background overlaps the inelastic scattering signal: We were unable to measure the scattering intensity near 0° for $D_2(v' = 1, j' = 4)$, and we were also prevented from measuring DCSs for $D_2(v' = 1, j' < 4)$.

Slow-Channel Contamination. The H atoms used in the collision are generated by photolysis of HBr, which may proceed by 2 channels that create H atoms with different speeds. Products formed in collisions with slow H atoms from the minor channel of HBr photolysis will have a different mapping from the measured speed to the center-of-mass scattering angle and may distort the DCS if a subtraction is not performed. Such corrections are expected to be small, however. Only approximately one-sixth of the H atoms produced by HBr photolysis are from the slow channel (22). These slower moving H atoms are less likely to encounter a D_2 molecule during the time allowed for the reaction, and, in general, these collisions have smaller cross-sections compared with their more energetic counterparts. Only a few percent of the measured signal is expected to arise from slow-channel H atoms. If contamination is present, it should be spread over a smaller range of angles for higher v': for $D_2(v' = 1, j' = 8)$ the allowed slow-channel speed range overlaps 83% of the fast-channel speed range, but for $D_2(v' = 3, j' = 8)$, any potential slow-channel contamination can overlap only 44% of the fast-channel speed range (see Table S1). Within experimental error, however, the $j' = 8$ DCS is identical for all vibrational states studied (see Fig. 2). Similarly, we see no significant differences between $D_2(v' = 1, j' = 4)$ vs. $D_2(v' = 2, j' = 4)$ or between $D_2(v' = 1, j' = 14)$ vs. $D_2(v' = 2, j' = 14)$. It is unlikely that slow-channel contributions, which would contaminate a different range of angles in each case, would exactly cancel out a dependence on the D_2 product vibrational state. We conclude that the qualitative trends should be minimally affected by contamination from the slow channel of HBr photolysis, although ideally, the slow-channel contribution should be measured and subtracted as in Koszinowski *et al.* (8).

Influence of Rotationally Excited Reactants. One final source of uncertainty to consider is the fact that the reactant D_2 is not perfectly cold and consists of roughly equal amounts of $j = 0$ and 2 (odd j' cannot contribute because of symmetry). The energies differ by only a small amount, 0.02 eV, and this value is included in the data analysis, but the dynamics may be subtly different for rotationless vs. rotationally excited D_2. One likely effect is a slight blurring at high values of j'. For example, our measurements of $j' = 14$ contain a mixture of $\Delta j = 14$ and $\Delta j = 12$, and the peak scattering angles may differ by a few degrees. The effect might be stronger and less predictable for low values of j'. For example, measurements of $j' = 0$ include collisions with rota-

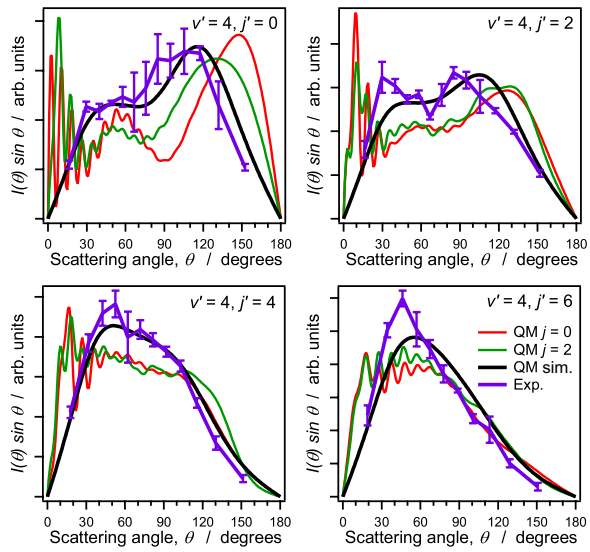

Fig. 4. Comparison of measured differential cross sections for $D_2(v' = 4, j' = 0,2,4,6)$ formed at $E_{coll} = 1.82$ eV (purple lines) with fully converged quantum mechanical calculations (black lines). Calculated contributions from $D_2(v = 0, j = 0)$ and $D_2(v = 0, j = 2)$ reactants are shown separately (red and green lines, respectively). The black lines are averages of the contributions from $D_2(v = 0, j = 0)$ and $D_2(v = 0, j = 2)$ weighted to match the fractions of these components present in the molecular beam and blurred to match the velocity resolution of the experiment. Error bars on the purple lines represent 1 standard deviation.

tional deexcitation. Also, quantum interference effects are known to occur for the reactive HD($v' = 3, j' = 0$) channel, but not for higher values of j' (23). Inelastic trajectories often cross the reaction barrier, and this effect becomes more important as v' increases (1). The DCS will likely be most sensitive to ill-defined initial conditions at high v' and low j', which is precisely where the most interesting bimodal features appear.

Comparison with QM Calculations. The measured DCSs for $D_2(v' = 4, j' = 0,2,4,6)$ are compared in Fig. 4 with the results of QM calculations. The cross-sections for $v' = 4$ are several times smaller than those for other vibrational manifolds, resulting in extremely weak signal levels. Furthermore, at high values of v' and low values of j' (where the DCS shows the strongest effects of barrier recrossing and quantum interference) quasiclassical calculations fail to provide quantitative agreement with experiments (16). For these reasons, the DCSs for $v' = 4$ should be the strictest test of the accuracy of both the calculation and the experiment.

Separate calculations were carried out for $D_2(v = 0, j = 0)$ and $D_2(v = 0, j = 2)$ reactants, and the results were weighted to match the fractions present in the experiment. The contributions of $j = 0$ and $j = 2$ to the DCS are shown in Fig. 4 along with the averaged result, which has been further blurred to match the velocity resolution of the experiment. For $D_2(v' = 4, j' = 0)$, rotational excitation of the reactant causes a significant shift in the position of the sideward-scattered peak, but for higher values of j' the inclusion of excited reactants causes only a slight correction. Contributions from rotational levels $j > 2$ of the reactant and from the minor channel of HBr photolysis are neglected. In all cases, close agreement is found between the experiment and the calculation (similar overall agreement is found for $v' = 1$–3 products as shown in Figs. S2–S4).

Forward-Scattering Is Ubiquitous. All of the measured DCSs contain a large peak in the forward-scattered direction. This fact extends our previous observation that o-$D_2(v' = 3, j' = 0$–$8)$ products are predominantly forward-scattered at $E_{coll} = 1.72$ eV: We show that this behavior is general for $v' = 1$–4, for values of j' as high as 14, and for a wide range of collision energies. Together with the striking similarities in the bimodal structures of the $v' = 3$ and $v' = 4$ DCSs, this evidence suggests that the tug-of-war mechanism dominates inelastic scattering over a broad range of conditions.

Dependence on v' and j'. Only small differences are apparent between the DCSs for $v' = 3$ and $v' = 4$, as shown in Fig. 2. To the extent that a trend can be identified, it appears that $v' = 4$ products are more back-scattered than $v' = 3$ products. Our QM calculations show evidence of transition-state recrossing, particularly for $D_2(v' = 3,4, j' = 0)$ products, and QCT calculations (1) have shown that the fraction of recrossing trajectories increases significantly with v'. No accurate QCT results are available yet for $v' = 4$ because of the small numbers of trajectories scattered into those quantum states. The experimentally observed trend, although weak, is consistent with the notion that low-impact-parameter recrossing trajectories play a somewhat larger role for $v' = 4$ than they do for $v' = 3$.

Interestingly, although the bimodal feature for $j' \leq 4$ is observed only for high v', there is otherwise very little dependence of the DCS on Δv. Previous work (15) indicated that the rotational-state distributions have a very weak dependence on Δv; one might reasonably expect to observe larger changes in the DCS, a more sensitive probe of the dynamics, for such large differences in the amount of energy transferred into vibration (recall that the energy of a quantum of D_2 vibration is approximately equal to the height of the reaction barrier on the minimum energy path), but this is not what we observe. Hints of this counterintuitive behavior were also found by Serri *et al.* (24, 25) when they measured DCSs for Na_2 + Ar inelastic scattering and found that the peak scattering angle shifted by only 10° between $\Delta v = 0$ and $\Delta v = 1$ at large Δj. The vibrational spacing of Na_2 is small, and its interaction with Ar is almost totally repulsive. In the H + D_2 system, much more energy is transferred into vibration, and we believe that attractive forces are crucial for explaining how products with high vibrational excitation are scattered in the forward direction; nevertheless, there may be a connection between our observations and the work of Serri *et al.*

Given the overall weak dependence on v', it is puzzling that for low j', we see a striking contrast between $v' = 1,2$ and $v' = 3,4$. This behavior is most directly compared for $j' = 4$, which was measured for all 4 vibrational manifolds (Figs. 1 and 2). The forward-scattered peak is significantly narrower for $v' = 1,2$ than for $v' = 3,4$. Much information could be gained by comparing trends in the DCSs for $j' = 0$ and 2, which are more clearly bimodal than $j' = 4$, but because of strong background, we were able to measure these DCSs only for $v' = 3,4$.

Dependence on Collision Energy. Only a small dependence on the collision energy is evident over the range $1.58 \leq E_{coll} \leq 1.94$ eV for the $v' = 3$ DCSs, as seen in Fig. 3. Although the trend is barely more significant than the statistical error, the slight shift toward forward-scattering with increasing collision energy is consistent with the participation of larger impact parameters. We did not examine the collision energy dependence of the other vibrational manifolds, but we expect that any trends would be weak, as they are for reactive scattering over a similar range of energies (8). Further evidence is provided by the close agreement between $v' = 1$ and $v' = 2$ DCSs, despite the fact that the former were measured by using a single laser and thus have slightly different collision energies for each j', whereas the latter are all fixed at $E_{coll} = 1.72$ eV. The comparison in Fig. 2 between $v' = 3$ and $v' = 4$ at collision energies differing by 0.1 eV should not be problematic. If both sets of DCSs had been measured at the same collision energy, the shift toward backward-scattering for $v' = 4$

might be slightly more pronounced; this would only strengthen the trend that is already apparent.

Conclusions

This study presents a thorough overview of vibrationally inelastic H + D_2 scattering. We have measured 19 DCSs covering a wide range of $D_2(v',j')$ product quantum states and collision energies. For all vibrational manifolds studied, $v' = 1$–4, the products are scattered predominantly into the forward hemisphere. This result is in contradiction to conventional wisdom, which says that the grazing collisions at large impact parameters that lead to forward-scattering should not be able to excite vibration in the target. We suggest that the recently discovered tug-of-war mechanism (16) is responsible for generating forward-scattered D_2 with vibrational excitation.

In general, the majority of the scattering intensity appears in a broad peak near 30°. This peak is narrower and more forward-scattered for low values of j', and the distribution broadens and shifts toward sideward-scattering as j' increases. For $j' \leq 4$, a second peak appears, but this feature is only apparent for $v' = 3$ and 4. In contrast, the dependence of the DCS on v' is surprisingly weak, and for $j' > 4$, there is essentially no dependence on v' within the experimental resolution. The attractive well is shallower for shorter equilibrium D_2 bond lengths (lower vibrational states), but we see dominant forward-scattering even for small Δv. Judging by the ubiquity of forward-scattering in the H + D_2 system, we suggest that other chemical systems with attractive forces between the collision partners may exhibit similar behavior.

The dependence of the inelastic scattering DCS on the collision energy appears to be generally weak over the range $1.58 \leq E_{coll} \leq 1.94$ eV. This result is consistent with what has been seen for the reactive channel at similar collision energies (8). Further measurements of 1 quantum state in particular, $D_2(v' = 3, j' = 0)$, would be of interest because this channel is dominated by recrossing trajectories (16), and the related reactive scattering process that generates $HD(v' = 3, j' = 0)$ exhibits quantum interference effects that depend strongly on the collision energy (26). Using a similar experimental method, we recently confirmed QM calculations for the reactive channel to a high level of detail (9), so extending such collision energy studies to the $D_2(v' = 3, j' = 0)$ inelastic channel should be feasible.

The close agreement between the DCSs measured here and what was seen previously for o-$D_2(v' = 3, j')$ suggests that a similar mechanism is at work, but this question cannot be answered definitively by experiments alone. New QM calculations agree well with experimental findings and corroborate the observed forward-scattering. Some of the DCSs (e.g., $v' = 3,4$, $j' = 0$) also show strong evidence of transition-state recrossing, in the form of E–θ ridges similar to those observed in the DCSs of the HD + D product channel (26). Nevertheless, QM calculations offer less insight into the mechanisms of inelastic scattering than quasiclassical calculations. No accurate QCT studies have been carried out as yet for $v' = 4$ because of the small numbers of trajectories scattered into these quantum states; it is clear that more theoretical work will be required to unravel this unexpected behavior in the benchmark H + D_2 system.

Overall, we have found a mechanism for vibrationally inelastic energy transfer. This tug-of-war mechanism is supported by experiments, QM calculations, and QCT calculations. We discovered this mechanism by looking at the H + D_2 system, which is one of the simplest and best-studied collision systems and has long served as a benchmark for developing deeper understanding of collisional dynamics. The mechanism appears to be the dominant one for vibrational energy transfer in this system. We observe forward-scattering for all quantum states and collision energies studied. It seems likely that this mechanism will be found to apply to other vibrationally inelastic scattering systems that undergo frustrated reactions in which strong attractive forces develop in the course of the collision process.

Methods

Experimental. The setup is similar to what has been described recently (8, 21, 22). A mixture of 3% HBr in D_2 ($P \approx 1.3$ bar) is introduced through a 10-Hz pulsed valve into a vacuum chamber. The reactants undergo internal and translational cooling in a supersonic expansion, and most of the D_2 is prepared in ($v = 0, j \leq 2$) (22). Two linearly polarized, tunable UV laser pulses ($\Delta\tau \approx 5$ ns) intersect the molecular beam at right angles. Each pulse is generated by frequency tripling the output of a dye laser pumped by the second harmonic of a Nd:YAG laser. The tripled light is separated by using dichroic mirrors and focused onto the molecular beam by a lens ($f = 50$ cm in 1 case, $f = 60$ cm in the other). The laser beams are counterpropagating, so that the 2-color Doppler-free signal from static H_2/HD/D_2 can be used to optimize the experimental conditions against near-zero background (8).

The reaction is initiated by photolyzing HBr with a pulse of laser light ($200 \leq \lambda \leq 216$ nm, $E_{pulse} \approx 300$ μJ) to produce monoenergetic H atoms with a well-defined spatial anisotropy. The energy resolution is limited by the rotational energies of the HBr and D_2 reactants in the molecular beam, which contribute 0.016 and 0.019 eV of broadening, respectively. The major photolysis channel yields H atoms and ground-state Br ($^2P_{3/2}$), but a minor channel can also produce spin-orbit excited Br* ($^2P_{1/2}$). The minor pathway has a branching fraction of $\Gamma \approx 0.18$ (22) and is termed the slow channel, because the spin-orbit excitation energy $\Delta E_{SO} = 0.45$ eV is no longer available for translation of the H atom. For the H + D_2 reaction, this fact leads to a small contamination at a collision energy that is less than the nominal value by 0.36 eV.

Collisions with H atoms cause some of the initially cold D_2 molecules to become rovibrationally excited; nascent o-$D_2(v' = 1$–$4, j')$ is state-selectively probed via [2 + 1] REMPI on the Q branches of the $E,F\,^1\Sigma_g^+ - X\,^1\Sigma_g^+$ transitions ($208 \leq \lambda \leq 227$ nm, $E_{pulse} \approx 300$ μJ). These molecules move quickly in the laboratory frame ($v \approx 10^3$ to10^4 m s^{-1}), so the wavelength of the probe laser is scanned over the Doppler profile to avoid bias against molecules with large velocity components parallel to the laser propagation direction. The resultant D_2^+ ions are formed in the extraction region of a Wiley–McLaren time-of-flight mass spectrometer. These ions are accelerated by extraction and acceleration voltages of $V_{ext} = -15$ and $V_{acc} = -60$ V, respectively, toward a time- and position-sensitive microchannel plate/delay line anode detector (DLD-120; RoentDek) whose output is analyzed to determine the 3-dimensional velocity of each incident ion.

The delay between the photolysis and probe pulses is $\Delta t = 10$ ns; at this delay, the $D_2(v', j')$ product signal is still increasing linearly with time. This fact suggests that the delay time is short enough to avoid any bias against fast-moving products that may fly out of the laser focal volume before they can be detected. We expect single collisions between H and D_2 under all reasonable experimental conditions, and we found no evidence that the $D_2(v', j')$ population is depleted by secondary collisions at this short delay time. Secondary collisions could also decrease the translational energy of D_2 products without altering their rovibrational quantum states. We did not observe these signatures at too-slow speeds, providing further evidence that we are in the single-collision regime.

Ideally, H atoms would be produced only during the initial photolysis laser pulse. In reality, the probe laser is also capable of photolyzing HBr and subsequently ionizing D_2 products within the same laser pulse. This background does not depend on the photolysis laser and is subtracted by altering the delay so that the probe pulse precedes the photolysis pulse on an every-other-shot basis. The Boltzmann ratio for $v = 0 : v = 1$ at 298 K is $\approx 10^6$:1, and it is well known that supersonic expansions are less effective at cooling vibration than translation or rotation because of the longer relaxation times for vibration (27). Vibrationally excited $D_2(v = 1)$ reactants can be detected in the molecular beam. This background appears at slow speeds and in some cases contaminates the signal for $v' = 1$ products. Because vibrationally excited reactants comprise a tiny fraction of the D_2 in the molecular beam, they should not affect measurements of products with $v' \neq 1$.

The photoloc method (photoinitiated reaction analyzed by the law of cosines) (28), is used to map the observed laboratory-frame product speeds $|v_i|$ into unique center-of-mass scattering angles θ_i. This allows us to convert the measured speed distribution into the differential cross section, $I(\theta)$. Each experiment is repeated between 3 and 7 times and the standard deviation used to estimate the overall error. To ensure reproducibility, several experiments were repeated a few weeks apart; good agreement was found in each case.

The small number of events remaining after background subtraction (between 400 and 1,000 events in a single scan) poses a challenge when centering the 3-dimensional image to correct for slight differences in laser alignment from 1 day to the next. These experiments also suffer from large background, especially at slow laboratory speeds. In a previous experiment on reactively scattered HD(v', j') using the same method (8), the largest single source of blurring was the $\approx$160-m s^{-1} photoionization recoil of the REMPI detection scheme, with additional blurring caused by the finite laser focal volumes and the imperfect cooling of reactants in the molecular beam. In that experiment, the overall speed resolution ranged between 200 and 400 m s^{-1}, leading to an average of 28 angles in the DCS. Although the recoil is smaller in the present experiment ($\approx$100 m s^{-1}), the angular resolution is slightly worse at an average of 16 distinct angles. The decreased resolution is caused by a combination of worse signal-to-background ratios and a decreased dynamic range of allowed laboratory speeds; together, these factors force us to choose larger bins to attain reasonable statistical error bars.

Theoretical. The quantum calculations were carried out by using the wave packet method of ref. 29, which was modified to treat state-to-state inelastic scattering. The H_3 potential energy surface of Boothroyd *et al.* (30) was used. The propagation of the wave packet was partitioned into 3 stages, corresponding to the entrance, strong-interaction, and exit stages of its time evolution. The strong-interaction part of the calculation included a portion of the 2 HD + D product channels, which allowed the wave packet to describe correctly the recrossing dynamics. The wave packet was represented on a grid of reactant-arrangement Jacobi coordinates (R,r,θ), with radial grid separations of 0.11 a.u. (ΔR), and 0.09 a.u. (Δr), and a total of 45 G-Legendre angular grid points. The calculations were repeated for all partial waves in the range J = 0–55, with the maximum projection of J on the intermolecular axis set to 20. These parameters were sufficient to yield state-to-state cross-sections converged to $<$5% over a continuous range of collision energies from 0.5 to 2.3 eV.

ACKNOWLEDGMENTS. This work was supported by the National Science Foundation under Grant CHE 0650414 (N.T.G., J.Z., K.K., and R.N.Z.). F.B. and S.C.A. acknowledge a grant from the U.K. Engineering and Physical Sciences Research Council.

1. Aoiz FJ, Bañares L, Herrero VJ (2005) The H+H_2 reactive system. Progress in the study of the dynamics of the simplest reaction. *Int Rev Phys Chem* 24:119–190.
2. Teslja A, Valentini JJ (2006) State-to-state reaction dynamics: A selective review. *J Chem Phys* 125:132304.
3. Yang X (2007) State-to-state dynamics of elementary bimolecular reactions. *Annu Rev Phys Chem* 58:433–459.
4. Kliner DAV, Adelman DE, Zare RN (1991) Comparison of experimental and theoretical integral cross sections for D+H_2(v=1,j=1)→HD(v'=1,j')+H. *J Chem Phys* 95:1648–1662.
5. Pomerantz AE, *et al.* (2004) Disagreement between theory and experiment in the simplest chemical reaction: Collision energy dependent rotational distributions for H+D_2→HD(v'=3,j')+D. *J Chem Phys* 120:3244–3254.
6. J. Zhang, *et al.* (2006) State to state to state dynamics of the *D*+H_2→H*D*+H reaction: Control of transition-state pathways via reagent orientation. *Phys Rev Lett* 96:093201.
7. Gustafsson M, *et al.* (2006) Observing the stereodynamics of chemical reactions using randomly oriented molecular beams. *J Chem Phys* 124:241105.
8. Koszinowski K, *et al.* (2007) Differential cross section for the H+D_2→HD(v'=1,j'=2,6,10)+D reaction as a function of collision energy. *J Chem Phys* 127:124315.
9. Goldberg NT, Zhang J, Miller DJ, Zare RN (2008) Corroboration of theory for H+D_2→D+HD(v'=3,j'=0) reactive scattering dynamics. *J Phys Chem A* 112:9266–9268.
10. Blais NC, Truhlar DG (1985) Product state distributions for inelastic and reactive H+D_2 collisions as functions of collision energy. *J Chem Phys* 83:2201–2206.
11. Gerrity DP, Valentini JJ (1985) Dynamics of inelastic H+D_2 collisions: Product quantum state distributions at 1.1 and 1.3 eV collision energy. *J Chem Phys* 83:2207–2213.
12. Valentini JJ, Gerrity DP (1986) State-to-state dynamics of the hydrogen-exchange reaction. *Int J Chem Kinet* 18:937–948.
13. Schechter I, Levine RD (1986) Dynamical stereochemistry of the hydrogen-exchange reaction—A computational study. *Int J Chem Kinet* 18:1023–1045.
14. Phillips DL, Levene HB, Valentini JJ (1989) Experimental study of the dynamics of the D+H_2 reactive and inelastic collisions below 1.0 eV relative energy. *J Chem Phys* 90:1600–1609.
15. Pomerantz AE, *et al.* (2004) Rovibrational product state distribution for inelastic H+D_2 collisions. *J Chem Phys* 121:6587–6590.
16. Greaves SJ, *et al.* (2008) Vibrational excitation through tug-of-war inelastic collisions. *Nature* 454:88–91.
17. Levine RD (1990) The chemical shape of molecules: An introduction to dynamical stereochemistry. *J Phys Chem* 94:8872–8880.
18. Hirschfelder J, Eyring H, Topley BJ (1936) Reactions involving hydrogen molecules and atoms. *J Chem Phys* 4:170–176.
19. Truhlar DG, Wyatt RE (1976) History of H_3 kinetics. *Annu Rev Phys Chem* 27:1–43.
20. Levine RD (2005) *Molecular Reaction Dynamics* (Cambridge Univ Press, Cambridge, UK), p 376.
21. Goldberg NT, Koszinowski K, Pomerantz AE, Zare RN (2007) Doppler-free ion imaging of hydrogen molecules produced in bimolecular reactions. *Chem Phys Lett* 433:439–443.
22. Koszinowski K, Goldberg NT, Pomerantz AE, Zare RN (2006) Construction and calibration of an instrument for three-dimensional ion imaging. *J Chem Phys* 125:133503.
23. Fernández-Alonso F, *et al.* (2000) Evidence for scattering resonances in the H+D_2 reaction. *Angew Chem Int Ed* 39:2748–2752.
24. Serri JA, *et al.* (1980) Observation of halos in rotationally inelastic scattering of Na_2 from Ar. *J Chem Phys* 72:6304–6306.
25. Serri JA, *et al.* (1981) Level to level differential cross sections for vibrationally-rotationally inelastic collisions of Na_2 with Ar. *J Chem Phys* 74:5116–5119.
26. Althorpe SC, *et al.* (2002) Observation and interpretation of a time-delayed mechanism in the hydrogen exchange reaction. *Nature* 416:67–70.
27. Kantrowitz A, Grey J (1951) A high intensity source for the molecular beam. Part I. Theoretical. *Rev Sci Instr* 22:328–332.
28. Shafer NE, Orr-Ewing AJ, Simpson WR, Xu H, Zare RN (1993) State-to-state differential cross-sections from photoinitiated bulb reactions. *Chem Phys Lett* 212:155–162.
29. Althorpe SC (2001) Quantum wavepacket method for state-to-state reactive cross sections. *J Chem Phys* 114:1601–1616.
30. Boothroyd AI, Keogh WJ, Martin PG, Peterson MR (1996) A refined H_3 potential energy surface. *J Chem Phys* 104:7139–7152.